A comprehensive photoabsorption, photoionization, and shake-up excitation study of the C1s cross section of benzene

Cite as: J. Chem. Phys. **113**, 7362 (2000); https://doi.org/10.1063/1.1290029
Submitted: 23 March 2000 . Accepted: 07 July 2000 . Published Online: 19 October 2000

E. E. Rennie, B. Kempgens, H. M. Köppe, U. Hergenhahn, J. Feldhaus, B. S. Itchkawitz, A. L. D. Kilcoyne, A. Kivimäki, K. Maier, M. N. Piancastelli, M. Polcik, A. Rüdel, A. M. Bradshaw, et al.

A comprehensive photoabsorption, photoionization, and shake-up excitation study of the C 1*s* cross section of benzene

E. E. Rennie
Fritz-Haber-Institut der Max-Planck-Gesellschaft, Faradayweg 4-6, 14195 Berlin, Germany and Max-Planck-Institut für Plasmaphysik, Boltzmannstr. 2, 85478 Garching, Germany

B. Kempgens and H. M. Köppe
Fritz-Haber-Institut der Max-Planck-Gesellschaft, Faradayweg 4-6, 14195 Berlin, Germany

U. Hergenhahn
Fritz-Haber-Institut der Max-Planck-Gesellschaft, Faradayweg 4-6, 14195 Berlin, Germany and Max-Planck-Institut für Plasmaphysik, Boltzmannstr. 2, 85748 Garching, Germany

J. Feldhaus,[a] B. S. Itchkawitz, A. L. D. Kilcoyne,[b] A. Kivimäki,[c] K. Maier, M. N. Piancastelli,[d] M. Polcik, and A. Rüdel
Fritz-Haber-Institut der Max-Planck-Gesellschaft, Faradayweg 4-6, 14195 Berlin, Germany

A. M. Bradshaw
Max-Planck-Institut für Plasmaphysik, Boltzmannstr. 2, 85748 Garching, Germany

(Received 23 March 2000; accepted 7 July 2000)

The absolute photoabsorption cross section of benzene (C_6H_6), encompassing the C $1s^{-1}$ $\pi^* e_{2u}$ resonance, the C 1*s* threshold, the satellite thresholds, and extending up to 800 eV, has been measured using synchrotron radiation. Measurements of the discrete absorption structure from below the C 1*s* ionization threshold have been performed at high resolution. In order to unambiguously assign all structure present in the photoabsorption cross section, C 1*s* photoelectron spectra were measured from the C 1*s* threshold region up to 350 eV along with satellite spectra. The C $1s^{-1}$ single-hole and the satellite cross sections have been derived in absolute units, and their angular distributions have been determined. Resonant and normal Auger spectra were taken on the main features of the photoabsorption and single-hole cross sections. From the best resolved photoelectron spectra the underlying structure in the asymmetric benzene photoelectron peak can be partly disentangled. The experimental data show that at least two vibrational modes play a role in the C 1*s* photoelectron spectrum. The behavior of the investigated shake-up structure closely resembles that of ethene and ethyne, where the satellite bands due to $\pi \rightarrow \pi^*$ excitations gain intensity towards threshold, an observation which may be attributed to conjugate shake-up processes. These processes lead to a significant contribution of the satellite intensity to the production of the absorption features traditionally assigned to the carbon shape resonances in benzene. An EXAFS analysis of the wide range oscillations present on the photoabsorption cross section has been performed, and reveals the C–C nearest-neighbor distance. © *2000 American Institute of Physics.* [S0021-9606(00)00937-5]

I. INTRODUCTION

Benzene (C_6H_6) is the prototypical aromatic hydrocarbon ring molecule. Synchrotron radiation gas phase photoabsorption and photoelectron studies of benzene[1–5] along with similar studies on ethane,[6–11] ethene,[7,12–17] and ethyne[7,18–20] have played a major role in understanding photoexcitations in hydrocarbons. Moreover, these studies together with theoretical investigations have also helped in the understanding of the transition from simple hydrocarbons to more complicated molecules and even polymers. High resolution spectroscopy has recently become a subject of some interest in the core level region because of the possibility now available of measuring the vibrational fine structure. The latter is a sensitive indicator of perturbations in the molecular photoionization continuum, such as double excitations and shape resonances. In molecules possessing equivalent core levels, the interaction of nearly degenerate electronic states by vibrations of a suitable symmetry, so-called vibronic coupling, is possible. The showcase example for this effect in core level photoionisation is the O 1*s* photoionization of CO_2.[21] While this example is now understood on a quantitative level,[22] only the conceptional framework exists for the treatment of vibronic coupling in molecules with more than two equivalent centers.[23] On the other hand it has been debated that in hydrocarbons the vibrational structure can be fully derived from localized changes in the pertinent bonds, and moreover that these changes could be taken from a small

[a]Present address: Hamburger Synchrotronstrahlungslabor HASYLAB am DESY, Notkestr. 85, 22603 Hamburg, Germany.
[b]Present address: Department of Physics, North Carolina State University, Raleigh, North Carolina, 27695.
[c]Present address: Department of Physical Sciences, University of Oulu, 90570 Oulu, Finland.
[d]Permanent address: Department of Chemical Sciences and Technologies, University ''Tor Vergata,'' 00133 Rome, Italy.

number of building block components, namely methane.[8,17] As such a procedure would be an obvious simplification in the treatment of vibrational excitations, it is interesting to test this procedure in a case where an influence of vibronic coupling is to be expected from the molecular symmetry.

Benzene is a planar unsaturated hexagon whose p_z orbitals form a delocalized electron ring, both above and below the carbon atom plane. The molecular orbital sequence of benzene in its ground state (D_{6h} symmetry) may be written as

$$(\text{core})\,(2a_{1g})^2(2e_{1u})^4(2e_{2g})^4(3a_{1g})^2(2b_{1u})^2(1b_{2u})^2(3e_{1u})^4(1a_{2u})^2(3e_{2g})^4(1e_{1g})^4 \quad {}^1A_{1g}.$$

The sequence of the core electrons may be written as

$$(1a_{1g})^2(1e_{1u})^4(1e_{2g})^4(1b_{1u})^2.$$

The absorption spectra of benzene both above and below the C 1s ionization threshold are quite rich in structure. However, previous cross section measurements[3,4,24–29] have failed to fully resolve the discrete resonance structure converging onto the K-shell threshold, and to unambiguously identify the continuum resonances.

High resolution photoelectron spectroscopy has been shown to be very helpful in the correct identification of features in the photoabsorption continuum.[6,7,12,30–33] Local maxima occur in the photoabsorption spectra of molecules in the continuum just above threshold. Such enhancements may be due to shape resonances, satellite thresholds, conjugate enhancement of satellite channels, and autoionization from doubly excited states. Measurement of the absolute $C\,1s^{-1}$ main line and satellite partial photoionization cross sections along with direct comparison to the absolute photoabsorption cross section, allows an estimation of the different contributions of the $C\,1s^{-1}$ single hole state and the various neutral and ionic excited states to the total cross section. Classification of the above-threshold features can then be achieved by separating the single hole contribution from the satellite channels.

In this article we attempt to unambiguously assign all structure present in the photoabsorption cross section between 284 and 800 eV and, in order to achieve this, have measured the absorption, single-hole, and satellite cross sections as well as Auger spectra and the resonant Auger spectrum on the first π^*-resonance. We have studied the vibrational excitation upon K-shell ionization and the shake-up satellites of benzene. The experimental and data analysis procedures are presented in Sec. II–III. In Sec. IV the prethreshold features in the absorption spectrum are discussed and assigned, while the continuum features are assigned during the discussion of the single-hole and satellite cross sections and the Auger spectra in Sec. VI and IX, respectively. Section V considers the vibrational structure in the photoelectron main line. Section VII contains an extended x-ray-absorption fine structure (EXAFS) analysis of the oscillations present in the high energy range of the photoabsorption cross section and reconsiders the problem of obtaining structural information from resonant features in the absorption or partial photoionization cross section. The Auger spectra and any subsequent consequences that can be drawn for the assignment of continuum features are discussed in Sec. VIII. Section IX investigates the photon energy dependent behavior of the shake-up satellites of benzene. Also in this section, the asymmetry parameter of main and satellite lines will be discussed, including some comments on the effects of nondipole terms in the photoionization amplitude.

II. EXPERIMENTAL DETAILS

Absolute measurements of the photoabsorption cross section were carried out on the HE-TGM-1 beamline[34] at the BESSY I synchrotron radiation source in Berlin and on the X1B undulator beam line[35] at the x-ray ring of the Brookhaven National Synchrotron Light Source (NSLS). The cross section was measured from 284 to 310 eV with a photon energy resolution of about 50 meV at the NSLS X1B beamline, and from 284 to ~800 eV with a photon energy resolution of approximately 1 eV at the BESSY I HE-TGM-1 beamline. The energy scale in both measurements was normalized by aligning the center of the first, sharp C 1s resonance to an energy of 285.2 eV, which was found in electron energy loss (EELS) measurements.[29]

The experimental apparatus for the photoabsorption measurements has been described in detail by Itchkawitz *et al.*[36] and will be mentioned here only briefly. It consists of two main parts. In the first part a compact arrangement of two grazing incidence mirrors is used to suppress unwanted stray light and components resulting from higher diffraction orders of the grating. The ratio of first- to second-order light behind the device is generally 100:1 or better. The actual measurements are carried out in a gas-phase absorption cell by measuring the photocurrent on meshes in front of and behind the absorption path. Normalization for the absorption function of the various optical elements is done by comparison to spectra recorded with an empty sample cell. The absolute absorption cross sections can then be extracted by use of the Lambert–Beer law.

The inner shell photoelectron spectra were measured on the NSLS X1B beamline. During this work, two separate benzene main line series were measured in separate beam times. One data set contained 21 main line spectra along with 21 satellite spectra measured at the same energies. The second main line data set contained 42 spectra, measured with higher statistics and a lower resolution than the first set, as well as several high statistic, high resolution benzene spectra

taken at 308 eV. The two main line series along with the satellite spectra were used to accurately determine the absolute value of the single hole cross section and its β parameters. In a further beamtime, more high statistic, high resolution main line spectra of benzene were taken at 298 eV along with the well-known C $1s$ spectrum of carbon monoxide, to disentangle the excited vibrational modes.

The synchrotron radiation intensity was monitored by measuring the photocurrent on a stainless steel plate. The sample pressure was recorded by a capacitance absolute pressure gauge mounted immediately before the gas inlet, and was kept constant by a stepper motor driven valve. All main line spectra were taken alternately with Ne $2p$ photoelectron spectra to normalize for variations in the quantum efficiency of the beam monitor due to, e.g., absorption of sample gas molecules and for variations of the photon intensity at the point of interaction caused by changes of the beam position.

The photoelectron spectrometer used was a stationary, angle-resolving ''magic-angle'' cylindrical mirror analyzer (CMA), which is described in detail elsewhere.[37] One of the main features of this spectrometer is that it allows one to determine the asymmetry parameter β and the total photoelectron intensity, independent of β, at the same time. This is accomplished by mounting the CMA such that the incident beam passes along its rotational axis. The photoelectrons emitted in the reverse direction into the analyzer at an angle of 54.7° with respect to the light propagation axis are registered with an eight-fold symmetric position-sensitive detector anode. Within the dipole approximation, the angular distribution can be calculated from the difference in the signal intensity between anode sectors oriented within and perpendicular to the orbit plane of the storage ring, while the total cross section is proportional to the signal summed up over all anode sectors. Some account of the influence of nondipole interaction terms within this geometry is given below and in a forthcoming publication.[38]

The photoelectron kinetic energy bandwidth is determined by the CMA pass energy. The pass energy is typically kept constant for a related series of data. The effect of strong retardation or acceleration of the photoelectrons was deduced from measurements of neon $(2s)$ and argon $(2p)$.[33] The resolution can then no longer assumed to be a constant factor of the pass energy, but varies as a function of the photoelectron kinetic energy.

The entrance and exit slit settings of the spherical grating monochromator were 70 and 50 μm for the first main line series, consisting of 21 spectra, and the satellite spectra, which when coupled with a pass energy of 20 eV corresponds to a total resolution of 230 meV. The second main line series consisting of 42 spectra was measured with 100 μm slits and 20 eV pass energy corresponding to a total energy resolution of 330 meV. The high resolution measurements at 298 and 308 eV were measured with pass energies of 7.5 eV and, entrance and exit slit settings of 20 and 15 μm, respectively giving an overall energy resolution of 60 meV. All of the main line spectra were accumulated to 150 000–400 000 counts; the energy channel width was chosen to match the overall resolution and, for example, was 5 meV for the high resolution data taken at 298 eV.

III. DATA ANALYSIS

After normalization to light intensity, target gas pressure, and the transmission function of our analyzer, the main lines of the photoelectron spectra were analyzed in least-squares fits. In the line shape model, besides the contributions due to PCI,[39,40] an empirically determined apparatus profile, which has a slightly larger width towards the high-energy side,[33] was also taken into account. The areas of the main line and satellite contributions obtained for different photon energies as outlined above, were in turn normalized by the Ne $2p$ calibration measurements. For this the Ne $2p$ partial photoionization cross section[41] has to be used, but in fact it is only the slope of the curve in the photon energy region of interest that is of importance. The C $1s$ partial cross sections and satellite contributions were then obtained by scaling to the absolute photoabsorption data, as described in our previous publications.[19,30–32]

The high resolution spectra measured at 298 eV were recorded alternately with carbon monoxide C $1s$ spectra to ensure identical experimental conditions. These spectra were fitted along with the high resolution spectra taken at 310 eV and a sudden limit spectrum at 352 eV. The fit used a least-squares fit procedure with suitable parameters coupled between the various spectra, such as the instrumental profiles, the lifetime broadening, and the Franck–Condon factors.

IV. ABSOLUTE PHOTOABSORPTION CROSS SECTION

Despite the importance of the molecule, we are aware of only two absolute photoabsorption studies of benzene in the soft x-ray region. Akimov *et al.*[28] reported a spectrum covering a photon energy range of 25 eV around the C–K ionization threshold together with some additional data points obtained by line sources, and an EELS spectrum converted to absolute units obtained by Hitchcock *et al.* (unpublished data presented by Piancastelli *et al.*).[3] Therefore, we have measured the absolute photoabsorption cross section of benzene over a wide energy range, sections of which are shown in Figs. 1–3, 5, and 7. Table I contains the absolute values of the photoabsorption cross section between 300–800 eV in 25 eV steps. Part of the spectrum, above the C $1s$ ionization threshold between 290 and 350 eV, was published by Kempgens *et al.*[1] to illustrate the assignment problems in connection with shape resonances (see below), but was not discussed in detail. While the EELS data are in quantitative agreement with our results, the earlier measurements of Akimov *et al.*, with a reported accuracy of 20%, resulted in cross sections 20%–30% lower.[28] A more detailed discussion of our experimental procedure including error estimates will be published by Kempgens *et al.*[42]

The previous absolute photoabsorption measurements and the additivity data of Henke *et al.*[43] were not able to resolve the rich structure both below and above the C $1s$ ionization threshold. Relative cross section measurements[4,24–27,29] have succeeded in identifying the most promi-

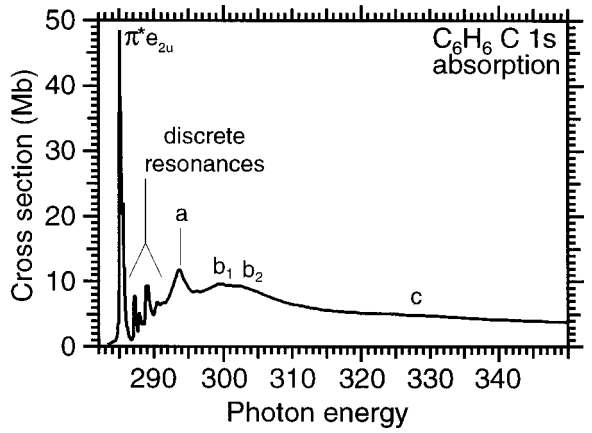

FIG. 1. Absolute photoabsorption cross section of benzene. The spectrum was measured between 284–310 eV on the NSLS X1B beamline and between 310–800 eV on the BESSY I HE-TGM-1 with energy resolutions of 50 and ~1 eV, respectively.

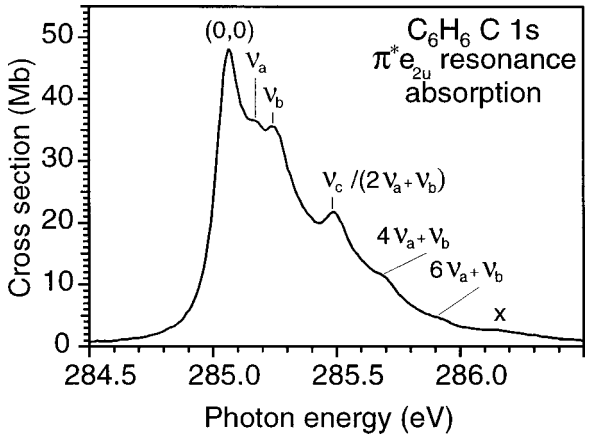

FIG. 2. Absolute photoabsorption cross section of benzene over the C $1s^{-1}\pi^*e_{2u}$ resonance.

nent features, but there still exists some uncertainty concerning their assignment. Several structural features can be identified in the cross section: (1) the C $1s^{-1}\pi^*e_{2u}$ excitation at ~285 eV,[24] (2) a region of discrete resonance excitations between 286.5 and 290 eV, a collection of previous assignments can be found in Ref. 44, (3) a relatively sharp rise to a maximum around 294 eV, labeled ''*a*,'' just after the C 1*s* ionization threshold at 290.42 eV,[45] (4) the features labeled ''b_1'' and ''b_2'' around 300 eV, and (5) a broad maximum labeled ''*c*'' between 320 and 340 eV. Features (1)–(4) have been observed previously with poorer resolution, except for the high resolution photoabsorption measurements of the C $1s^{-1}\pi^*e_{2u}$ resonance taken by Ma *et al.*[4] The feature labeled ''*c*'' has not been previously observed in gas-phase photoabsorption spectroscopy. This feature is a clearly visible part of the EXAFS oscillations present in the photoabsorption cross section, as we will show below.

TABLE I. Absolute photoabsorption cross section, energies between 284 and 350 eV (can be seen in detail in Figs. 1–5).

Photon energy (eV)	Cross section (Mb)
300	9.592
325	5.015
350	3.843
375	3.447
400	2.989
425	2.527
450	2.152
475	1.917
500	1.724
525	1.584
550	1.464
575	1.326
600	1.213
625	1.145
650	1.129
675	1.112
700	1.097
725	1.086
750	1.073
775	1.065
800	1.055

The features ''*a*,'' ''b_1,'' and ''b_2'' have traditionally been designated as shape resonance (Refs. 25, 27, 44, and references therein). However, recent publications about other simple unsaturated hydrocarbons have shown that above the satellite thresholds the energy dependence of the satellite intensities may produce broad maxima in the photoabsorption cross section that cannot be distinguished from a shape resonance in absorption measurements.[1,7] Therefore, we will discuss the dependence of the total photoabsorption cross section across features ''b_1'' and ''b_2'' together with the respective main line and satellite partial cross sections in Sec. VI.

Structure in the photoabsorption cross section, just above the C 1*s* ionization threshold and below the satellite thresholds could be due only to shape resonances and excitation into doubly excited states. Hence Auger spectra were taken on the C $1s^{-1}\pi^*e_{2u}$ resonance, ''*a*,'' in between ''*a*'' and ''b_1,'' ''b_1'' and in the sudden limit in order to obtain more information on the processes involved in the formation of resonance ''*a*,'' as described in Sec. VIII.

Figure 2 shows the absolute photoabsorption cross section of the C $1s^{-1}\pi^*e_{2u}$ resonance, between 284.5 and 286.5 eV. The observed structure is in very good agreement with that of Ma *et al.*,[4] except for a shift of 350 meV towards lower absolute excitation energies probably caused by the adoption of a different calibration procedure. High resolution measurements of both benzene and deuterated benzene were reported by these authors. They commented on the first four peaks, (0,0), ν_a[105(10) meV], ν_b[180(15) meV], and ν_c[420(15) meV]. A comparison between the hydrogenated and deuterated benzene spectra revealed isotopic shifts which suggested excitations of the C–H bond for ν_a and ν_c. However, ν_b exhibited no isotopic shift indicating an excitation of the aromatic carbon ring. The present results yield values, relative to the (0,0) peak, which lie well within the error bars quoted by Ma *et al.* On careful examination of the spectrum three further peaks can be seen, the first two peaks are at energies which correspond to $(4\nu_a+\nu_b)$ and $(6\nu_a+\nu_b)$. As the $(2\nu_a+\nu_b)$ excitation would lie underneath the ν_c excitation this tentative assignment seems reasonable.

The symmetries and neutral ground state energies of the benzene vibrations have been summarized elsewhere (Refs. 2, 46, and references therein), frequencies for the two totally symmetric ground state vibrations of 123 meV (ν_1) and 395 meV (ν_2) were reported. Comparing the ground state vibrations with the frequencies found for the excited state may give reasonable suggestions for ν_a and ν_b, e.g., the $\nu_{10}e_{1g}$ C–H bend (104.9 meV) could correspond to ν_a and the $\nu_{19}e_{1u}$ ring stretch and deformation (185.2 meV) could correspond to ν_b. There are a number of vibrational modes, including the $\nu_2 a_{1g}$ C–H stretch, with energies of approximately 390 meV with a C–H stretch characteristic which may correspond to ν_c. However the shift of 30 meV between ν_c and the highest energy vibrations may indicate that similar shifts could be present in the ν_a and ν_b excitations. A similar tentative assignment of the vibrational structure found within the C $1s^{-1}\pi^* e_{2u}$ resonance has been given by Ma *et al.* They assigned ν_a to one or several out-of-plane C–H bends, ν_b to a nontotally symmetric ring stretch, and ν_c to a C–H stretch.

The plausibility of the above assignment of the vibrational fine structure in benzene is corroborated by a comparison with the theoretical investigations on the C $1s^{-1}\pi^*$ resonance of ethene.[14,47] In ethene the main two peaks are at ~0.2 and ~0.5 eV higher energies than the (0,0) peak which is similar to the relative energies of ν_b and ν_c shown in Fig. 2. Another similarity between the π^*-resonance in ethene and benzene is the presence of excitations corresponding to combinations of multiples of the two main peaks. For ethene, the vibrational structure in the π^* resonance has been explained by excitation of the totally symmetric C–C and C–H stretching vibrations, the antisymmetric counterpart of the C–H stretching mode, and several out-of-plane torsional vibrational modes. The nontotally symmetric modes are excited by vibronic coupling. Two qualitatively different mechanisms for this have been revealed, namely coupling between the two core-excited species of *gerade* and *ungerade* symmetry, respectively, and coupling between a manifold of effective valence-excited states. The latter leads to the out-of-plane vibrations which are lowest in frequency among the vibrational modes excited. In a simplified picture, their effect is to smear out the gross structure of the spectrum given by the in-plane modes. Thus in benzene, the assignment of ν_a and ν_c to out-of-plane and C–H stretch modes, not necessarily totally symmetric, seems plausible. For ν_b the problem remains that it must be either identified with the totally symmetric ring stretch ν_1, which is 60 meV lower in energy in the neutral ground state, or with a nontotally symmetric ring stretch, which has no direct analogue in the ethene spectrum.

The third weak peak labeled ''*x*'' in Fig. 2, 1.1 eV higher than the (0,0) peak on the high energy flank of the C $1s^{-1}\pi^* e_{2u}$ resonance, does not correspond to any combination of multiples of the ν_a, ν_b, and ν_c vibrations. This peak can also be seen in both the benzene and deuterated benzene spectra of Ma *et al.*, where no isotopic shift was observed. This leads one to consider the theoretical prediction of Schwarz *et al.*,[44] who proposed a peak 0.8 to 1.5 eV higher in energy than the (0–0) excitation due to a reduction of symmetry of the molecule from $D_{6h} \rightarrow C_{2v}$. Using a single particle model they concluded that upon symmetry breaking the manifold of the 12 C $1s \rightarrow \pi^* e_{2u}(D_{6h})$ states will form two groups, the dipole allowed $1s(a_1) \rightarrow \pi^*(a_2)$ and the dipole forbidden $1s(a_1) \rightarrow \pi^*(b_1)$ excitations. In support of this argument Schwarz *et al.* cite the article by Akimov *et al.*,[28] where a splitting of 0.5 eV was resolved in pyridine, the $Z+1$ analogue of core-excited benzene. However, the second, forbidden, group of excitations were predicted to be over three orders-of-magnitude weaker than the dipole-allowed component. It is difficult to estimate the background contribution from the higher vibrational members of the (in C_{2v} symmetry) $1s(a_1) \rightarrow \pi^*(a_2)$ component to this very weak feature and hence this assignment is tentative. Hitchcock *et al.*[29] failed to report a splitting of the first EEL-excited π^*-resonance in benzene and fluorinated benzenes. However, they did report a splitting of approximately 1 eV seen in the first π^* resonance of their negative-ion spectra, due to lifting of the $1\pi^*$ orbital degeneracy in fluorobenzenes of sufficiently low symmetry.

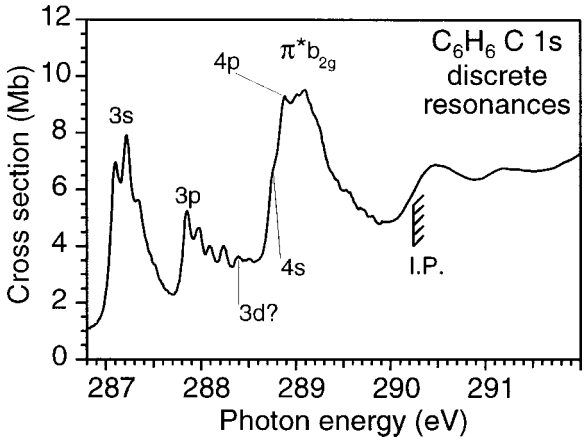

FIG. 3. Absolute photoabsorption cross section of benzene over the region of discrete resonances. The C $1s$ ionization threshold is at 290.42 eV (Ref. 45).

The region of discrete resonances can be seen in detail in Fig. 3. The $3s$ and $3p$ Rydberg resonances converging to the C $1s$ ionization threshold exhibit vibrational progressions with a spacing of 120 meV. This vibrational spacing is in good agreement with an excitation of the a_{1g} ring stretch, ν_1, with an energy of 123.3 meV. The positions of the $3d$, $4s$, and $4p$ Rydberg resonances have been calculated by Hitchcock *et al.*[24] using the Rydberg formulas with quantum defects obtained from valence spectra. A change in the shape of the $3p$ progression, marked $3d$?, coincides with the calculated position of the $3d$ Rydberg series. More convincing are the two shoulders on the C $1s^{-1}\pi^* b_{2g}$ resonance which correspond to the calculated positions of the $4s$ and $4p$ Rydberg resonances. The structure on the high energy tail of the C $1s^{-1}\pi^* b_{2g}$ resonance closely resembles that of a Rydberg series and is rather unlike the vibrational progressions exhibited by the C $1s^{-1}\pi^* e_{2u}$ resonance.

Schwarz *et al.*[44] has summarized all previous assignments of the pre-edge absorption spectra, which generally agree regarding the C $1s^{-1}\pi^* e_{2u}$, $3s$, and $3p$ resonances.

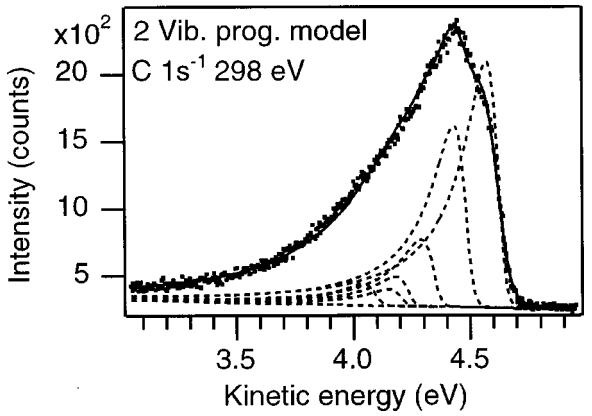

FIG. 4. C 1*s* photoelectron spectra of benzene measured at 298 eV photon energy fitted with a model containing two vibrational progressions. The dashed curves represent the individual vibrational states, while the full curve through the data points represents the final fit after summation and convolution with instrumental profiles.

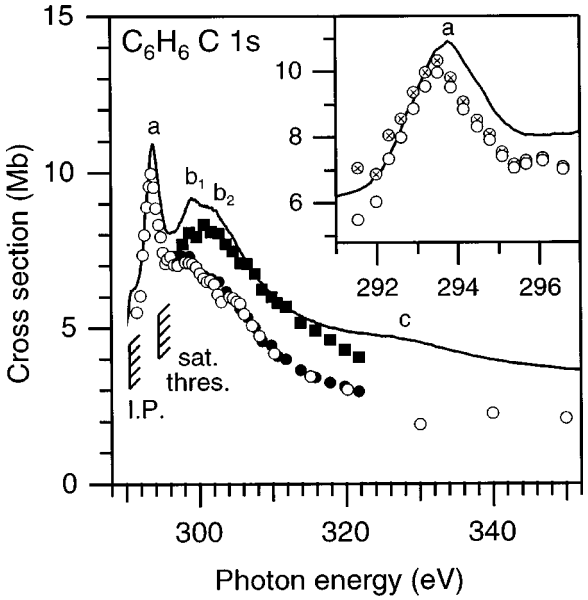

FIG. 5. The absolute C $1s^{-1}$ partial photoionization cross section. Key:—photoabsorption cross section (minus valence contribution), ● C $1s^{-1}$ main line photoionization cross section (1st data set containing 21 spectra), ■ C $1s^{-1}$ main line + satellites partial cross section (1st data set containing 21 spectra), ⊗ C $1s^{-1}$ main line photoionization cross section (2nd data set containing 42 spectra), ○ C $1s^{-1}$ main line photoionization cross section with PCI recapture correction (2nd data set containing 42 spectra).

For the peak between 289–290 eV the contributions of the $4s$, $4p$, and C $1s^{-1}\pi^* b_{2g}$ resonances could not be separated in earlier work, and varying assignments were given.

V. MAIN LINE PHOTOELECTRON SPECTRA

A high resolution C 1*s* photoelectron spectrum of benzene measured at a photon energy of 298 eV is displayed in Fig. 4. One can clearly see the asymmetry of the main line due to the underlying vibrational structure and the postcollision interaction (PCI).

This structure can be compared with an analysis of ethene and propene based on a fully localized building block model of hydrocarbon vibrations by Sæthre and coauthors.[17] These authors suggested that the main change upon C 1*s* ionization in a hydrocarbon is a shortening of the C–H bond, and that the amount of shortening is a universal quantity dependent only on the number of C–H bonds on the (strictly localized) site of ionization. Hence the vibrational excitation spectrum of benzene should look similar to the spectrum assigned to the middle atom (C2) in propene presented in Ref. 17 (one C–H bond). This spectrum consists mainly of the 0–0 component, with a weak shoulder due to the $\nu'=1$ excitation. Obviously this is not the case for our spectrum.

The shortcoming of the model described above is the obvious neglect of further vibrational progressions. We have therefore attempted an analysis with a model consisting of two progressions, following the suggestions in Ref. 17 as far as possible. That is, the linear coupling model was assumed for the Franck–Condon factors of both progressions, which are therefore given by a product of two Poisson distributions. A coupling parameter of $S=0.12$ for the C–H vibration was derived from the result presented for methane in Ref. 17 divided by four to account for the reduction in the number of C–H bonds. Anharmonicities were not taken into account. The overall intensity, the two vibrational frequencies, and the coupling constant of the second vibration were allowed to vary. This model produced an acceptable fit to the data, see Fig. 4. One of the two vibrational progressions had a frequency of 386 meV, which is typical for C–H stretching movements in hydrocarbons, while the other progression was found to be of a significantly lower frequency.

Thus we conclude that in benzene at least two vibrational modes are excited. Whether these two vibrational modes undergo C 1*s* core splitting due to energy differences between the different symmetry-adapted states, similar to acetylene,[19,20] cannot be determined within our fitting model. The ground state vibrations with an a_{1g} symmetry have energies of 123.3 meV, the ring stretch (ν_1), and 395.6 meV, the C–H stretch (ν_2). Further, we cannot rule out the excitation of nontotally symmetric modes which have similar energies to the ground state a_{1g} modes. From group theory considerations, modes of e_{1g}, b_{1u}, b_{2u}, e_{1u}, and e_{2u} symmetry may be induced via vibronic coupling. To distinguish which of these could play a role in this spectrum poses a serious theoretical problem and is beyond the scope of this article.

We note finally that the excitation of a ring deformation is also expected from the geometry of the C 1*s* ionized state of benzene in the core-equivalent approximation, $C_5H_6N^+$, which we have calculated using the GAMESS molecular structure program.[48] We found the optimized molecular geometry of $C_5H_6N^+$ to be planar, therefore in contrast to the C 1*s* $\rightarrow\pi^*$ excitation we expect no out-of-plane modes in the C 1*s* ionization of benzene.

VI. PHOTON ENERGY DEPENDENCE OF THE SINGLE-HOLE CROSS SECTION

The photoabsorption and C 1*s* single hole cross sections are depicted in Fig. 5 (the corresponding asymmetry parameter is discussed in Sec. IX, see Fig. 11). These data without the PCI correction have previously been published in Ref. 1.

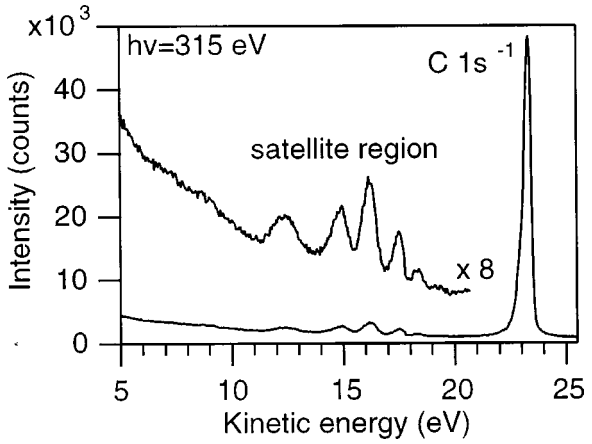

FIG. 6. C 1*s* photoelectron spectra of benzene at 315 eV photon energy, encompassing the main line and shake-up satellites.

In order to allow a scaling of the $C\,1s^{-1}$ cross section to absolute values a background due to valence excitations was subtracted from the photoabsorption spectrum. For very low kinetic energies the PCI profile used in our analysis[39,40] has a tail extending into ''negative'' kinetic energies. We have interpreted this as a finite probability for photoelectron recapture.[6] Points produced by subtracting the fraction of the intensity below the negative kinetic energy part of the curve are designated as recapture corrected (○) in this figure and the corresponding inset. While the uncorrected curve (⊗) represents the oscillator strength of the single-hole photoionization process, the corrected curve represents the intensity of the photoelectron signal actually observable in an experiment.

The sum of the intensity of the $C\,1s^{-1}$ main photoelectron line and its shake-up satellites (■) have been scaled to the absolute C 1*s* photoabsorption cross section at 307 eV photon energy, where the contribution from shake-off processes are expected to be negligible. We note, however, that the estimated error associated with this procedure could be as high as 10%. An example of a photoelectron spectrum containing the main line and shake-up satellites is shown in Fig. 6. In the inset to Fig. 5, the uncorrected data points of the single-hole cross section at low photon energies are placed slightly above the absolute photoabsorption curve. We believe this to be an artifact produced by an overall shift of the photon energy axis. We estimate an upper limit of ± 0.5 eV for the shift of all C 1*s* data points, with respect to the photoabsorption cross section, from our the calibration procedure. The possible influence of non-dipole effects is discussed in Sec. IX.

The sharp feature ''*a*'' in the photoabsorption cross section is reflected in the single-hole cross section (see Fig. 5). As mentioned in the introduction, such enhancements in the cross section below the satellite thresholds may be due to transitions into neutral doubly excited states, which populate the $C\,1s^{-1}$ singly ionized state by fast participator autoionization[7,19,30,49] or the presence of a shape resonance. Kempgens *et al.*[1] assigned ''*a*'' to a double excitation in analogy to the simple unsaturated hydrocarbons ethyne and ethene, and tentatively suggested a configuration of the type $1s^{-1}\pi^{-1}\pi^{*}$Ryd. We will return to the problem of assigning this feature in conjunction with the discussion of our resonant Auger spectra in Sec. VIII.

The most remarkable property that one can see in Fig. 5 is that the features ''b_1'' and ''b_2'' present in photoabsorption are almost absent in the single-hole cross section. These features are mostly caused by the shake-up satellite behavior immediately above threshold, as can be seen in the $C\,1s^{-1}$ main line + satellites partial cross section (■). Several of the satellites identified in the sudden limit[45] appear to be strongly enhanced by conjugate transitions about 5 eV above their respective thresholds. The details of the satellite structure will be discussed in Sec. IX. In the main line, only a very weak amplification in the 300–315 eV region can be imagined. This situation is similar to recent findings in ethyne, where Thomas *et al.*[20] using a combination of their *gerade/ungerade* symmetry-resolving C 1*s* data with our cross section curve[7] were able to quantify the main line enhancement due to the shape resonance at the maximum of the feature to be about 0.35 Mb, compared to a satellite intensity of 0.5 Mb.

Near-edge x-ray absorption fine-structure (NEXAFS) spectra of monolayer benzene have been measured on Pt(111) by Horsley *et al.*[27] and on Cu(110) by Bader *et al.*[50] The partial electron yield NEXAFS spectra measured at both normal and glancing x-ray incidence angles show that resonances ''b_1'' and ''b_2'' are enhanced in the normal incidence (90°) x-ray NEXAFS spectrum and are not present in the glancing incidence (20°) spectrum. This behavior is opposite to that of the $C\,1s^{-1}\pi^{*}e_{2u}$ resonance. From this, one must conclude that resonances ''b_1'' and ''b_2'' are of σ-symmetry. However, as can be seen in Fig. 5 and has been shown in the previous paragraphs, resonances ''b_1'' and ''b_2'' are caused mainly by the shake-up satellite behavior immediately above threshold. We are therefore confronted with a feature displaying the signature of a shape resonance in photoabsorption measurements while not being prominent in the main line cross section. This is in contradiction to the situation in N_2 and CO, for example, where there is a correspondence between absorption and main line shape resonances.[33,31] The correspondence of absorption and single particle cross section is an important cornerstone in the conventional picture of a shape resonance as an above threshold scattering state of high angular momentum produced by the molecular surroundings of the emitting atom. We have discussed this problem in a previous publication.[1] From our spectra, an approximate upper limit for the cross section enhancement due to this single-particle shape resonance in benzene is 0.5 Mb, compared to a satellite contribution of approx. 1.9 Mb at maximum.

In the energy region between 320 and 340 eV, marked ''*c*'' in the photoabsorption cross section, the data points are too scarce to determine whether this feature is present in the single-hole cross section.

The only other published single-hole partial cross section measurement has been made by Piancastelli *et al.*[3] using time-of-flight photoelectron spectroscopy. The decrease in intensity in their measurements between photon energies of 300 and 340 eV agrees fairly well with our results. Below

approximately 300 eV, however, their partial cross data display a decreasing intensity behavior towards threshold, although feature ''*a*'' may be seen as a local maximum. These early measurements were made at a bending magnet beamline with an excitation bandpass of ~2 eV width. Therefore, the increase due to the sharp feature ''*a*'' naturally will be washed out to some degree. Nevertheless, this explanation seems not sufficient to completely resolve the differences between their and our curves. The ratio of the Auger to main line intensity has been displayed by Piancastelli *et al.*,[3] and can be derived from measurements of our group.[51] While this ratio increases below 297 eV by 0.3 according to Ref. 3, it stays constant within 0.1 in our data. This points to a problem in the correction of the analyzer transmission in Ref. 3, which is notoriously difficult in electron time-of-flight spectroscopy, as the cause of the discrepancies between the two data sets. Since the fast Auger electrons will not experience a change in the transmission function, the increase in the Auger/C 1*s* ratio in Ref. 3 could be simulated partly by an underestimation of the C 1*s* line intensity, which when properly corrected for would bring their C 1*s* data points up higher. The shape of our main line cross section curve in relative units has been reproduced in an independent measurement.[51]

VII. EXAFS OSCILLATIONS

The fine structure in the benzene C 1*s* photoabsorption cross section was analyzed according to standard EXAFS procedures as follows: a smooth polynomial spline was fitted through the data in the energy range between 317 and 600 eV. The spline is shown as a dotted line in Fig. 7(a) and the corresponding normalized EXAFS oscillations in Fig. 7(b). The Fourier transform of the normalized oscillations is presented in Fig. 7(c). The chosen interval of the *k*-vector values was 2.8–7 $Å^{-1}$. For higher *k*-vector values the analysis was very sensitive to the parameters of the spline, thus yielding errors for the C–C distance well above 0.1 Å. The empirical C–C phase shifts taken from Ref. 52 ($\psi = 3.94 - 0.34k$) gave the distance of the nearest-neighbor carbon atoms in the molecule of 1.44 ± 0.05 Å. This value compares well with the literature value of 1.399(9) Å.[53] An attempt to extract the C–C bond lengths from extended inelastic electron scattering cross sections has been undertaken by Hollebone *et al.*[54] These authors arrive at a value of 1.36(4) Å.

It has been suggested by Stöhr and Bauchspiess[55] that shape resonances in *k*-space can be seen as a continuation of the EXAFS oscillations, and presented data for the diatomic molecule O_2 to demonstrate this. Our observed EXAFS structure unfortunately does not extend far enough in *k*-space to confirm their suggestion for benzene. A connection between resonances and EXAFS structure would also rationalize an earlier semiempirical correlation between shape-resonance positions as observed by photoabsorption or photoyield measurements and molecular bond-lengths, the ''bond-length-with-a-ruler'' relation (Ref. 56, see also Ref. 57 for a critical review). Taking the literature value of the bond length, and recalculating the shape-resonance position with the proportionality constant of Ref. 56 would place the

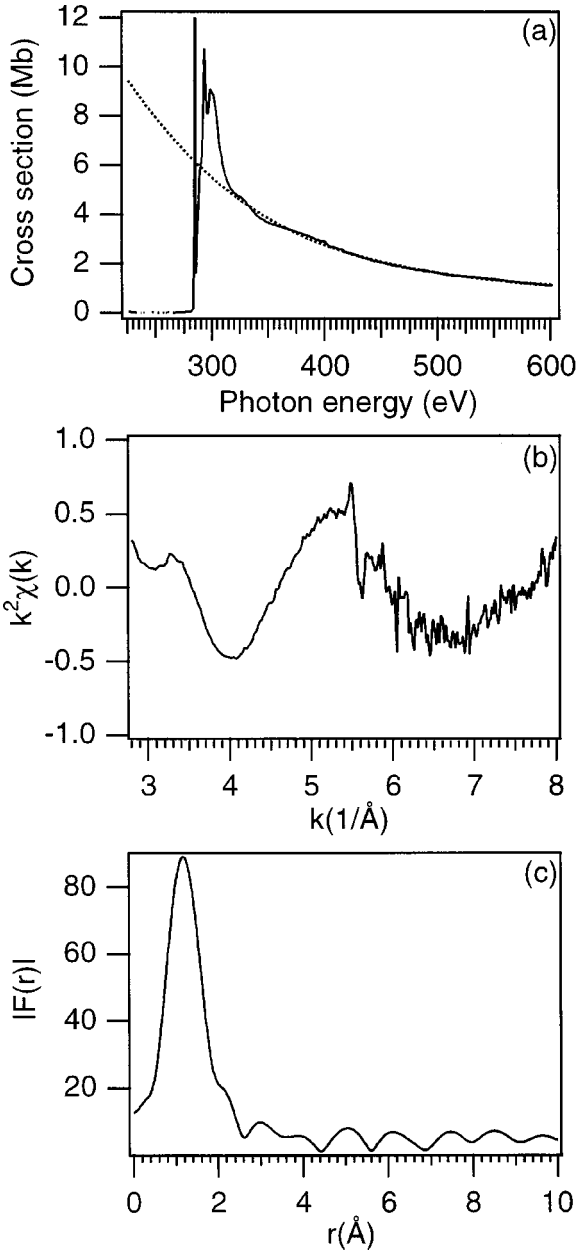

FIG. 7. (a) Polynomial spline fitted to the benzene absolute photoabsorption cross section between 317 and 600 eV; (b) normalized EXAFS oscillations; (c) Fourier transform of the normalized oscillations.

C_6H_6 C 1*s* shape resonance at ~9 eV above threshold, or at our feature ''b_1,'' which we have shown to be mainly of multiparticle character.

The fact that several resonances of σ symmetry are present in benzene cannot be accounted for in this approach, and the authors of Ref. 56 suggested averaging over the positions when different resonances of σ-symmetry are present. A potentially more satisfying procedure has been presented by Migal, who took into account the positions and lifetimes of all π^*- and σ^*-resonances to construct an *S*-matrix, which is then reproduced by an arrangement of muffin-tin potentials representing the scattering nuclei.[58] Another approach towards connecting the near-edge photoabsorption structure to molecular geometry of course is the use of numerical multiple scattering programs.[59,60] However, no results for benzene by any of these procedures are known to us.

VIII. AUGER PROCESSES IN C 1*s* IONIZATION

On resonance ''*a*'' both the photoabsorption and single-hole cross sections are enhanced. The results of NEXAFS spectra differ somewhat in the reported symmetry of this feature. While according to Horsley *et al.*[27] it is of σ-symmetry, Bader *et al.*[50] find this resonance under grazing and glancing angles, which suggests a mixed σ/π type. Unfortunately these facts still do not allow discrimination between the two possible processes, a double excitation or a shape resonance. Therefore Auger decay spectra were measured on the C $1s^{-1}\pi^*e_{2u}$ resonance, resonance ''*a*,'' resonance ''b_1,'' in between the latter two resonances, and in sudden limit conditions at 390 eV (see Fig. 8). These spectra are part of a series of benzene Auger and resonant Auger spectra to be published.[61]

The spectrum measured at the highest energy, 390 eV, is in good agreement with the Al Kα-excited spectrum of Siegbahn *et al.*[62] In the Auger spectra measured in the region of the resonances, the valence lines can be observed and have been joined in Fig. 8 by lines between the different spectra for ease of comparison. Comparison with He (II) spectra[63] shows that all of the valence lines can be seen quite clearly in the spectrum measured on resonance ''b_1.'' However, they are of low intensity due to the high photon energy of excitation. The Auger spectra at and between the resonances ''*a*'' and ''b_1'' are very similar. This corroborates our analysis of the single-hole cross section, which produces most of the additional oscillator strength making up feature ''*a*.'' The absence of valence line enhancement on all resonances except the first π^* was noted in resonant Auger spectra from solid benzene by Menzel *et al.*[26]

From the absence of additional features in the Auger spectrum recorded on resonance ''*a*'' we can limit the assignment to the following two possibilities: a double excitation of two electrons to non-Rydberg orbitals, or the traditional assignment as a shape-resonance. Resonant Auger decay of multiply excited states are know to influence the spectrum of the inner-valence region.[30,64] However, an excitation to $1\sigma_u^{-1}1\pi_u^{-1}1\pi_g^2$ has been identified in ethyne at an energy lower than the satellite maximum and C–C shape-resonance position, and was shown to lead to an increase in the single-hole cross section[19] as well as to a corresponding featureless amplification of the Auger spectrum.[49] Neutral double excitations decaying into the main line single-hole states have also been identified in valence photoionization of N_2.[65] In contrast to a non-Rydberg double excitation, a double excitation of the type $1s^{-1}\pi^{-1}\pi^*$Ryd is likely to undergo resonant Auger decay partially to $2h$-$1p$ states, which would appear at similar kinetic energies to the direct inner valence photoionization. An assignment as a $e_{1u}\sigma^*$ shape resonance is given by MS–Xα calculations by Horsley *et al.*[27] and the MBS-SCF calculations of Lucchese and Gianturco.[66] However, we note that this feature is uncharacteristically narrow for a shape-resonance.

Schwarz *et al.*[44] studied theoretically the energy levels of benzene core-excited and core-ionized states, and found strong mixing between the C $1s^{-1}\pi^*b_{2g}$ single particle excitation with doubly excited states resulting from $\pi-\pi^*$ shake-up. From these calculations they have predicted a resonant excitation of multiparticle character above the ionization threshold, which might be underlying the σ^* shape-resonance. Since the multiparticle state would acquire its oscillator strength from the $1s^{-1}\pi^*b_{2g}$ admixture,[44] this could explain the reports of both σ- and π-components in resonance ''*a*,''[50] and therefore seems the most plausible assignment to us.

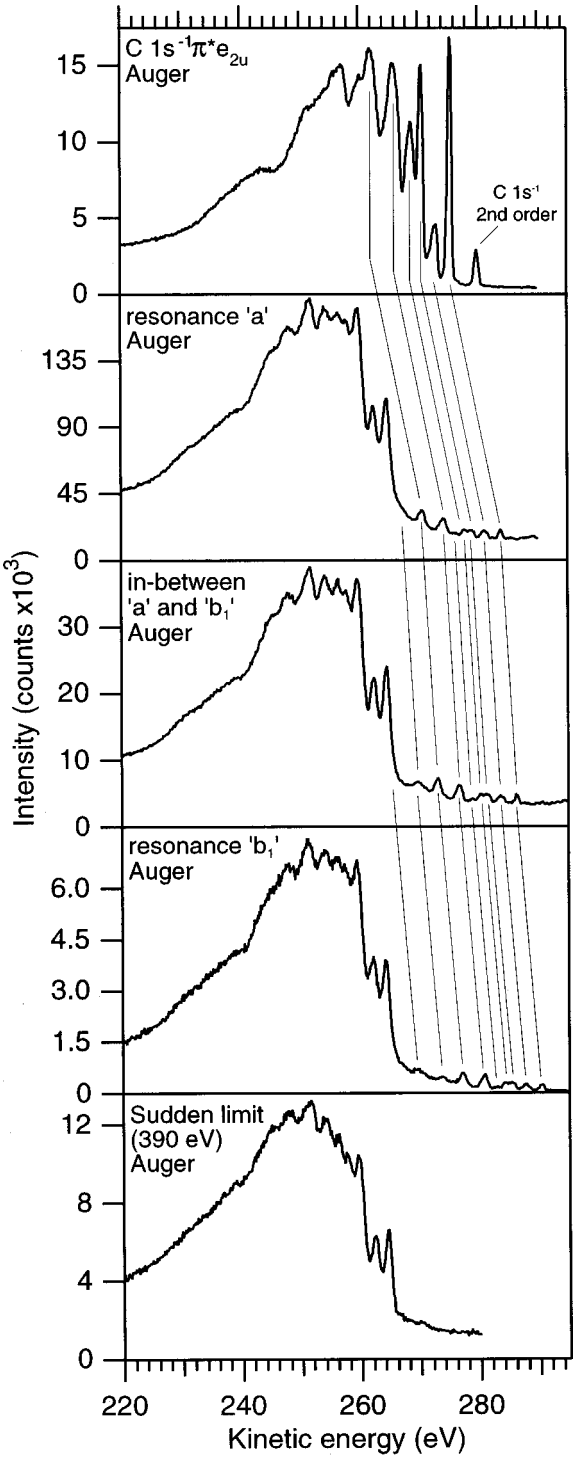

FIG. 8. Auger electron decay spectra of benzene. The lines trace individual valence states across the different Auger spectra to guide the eye.

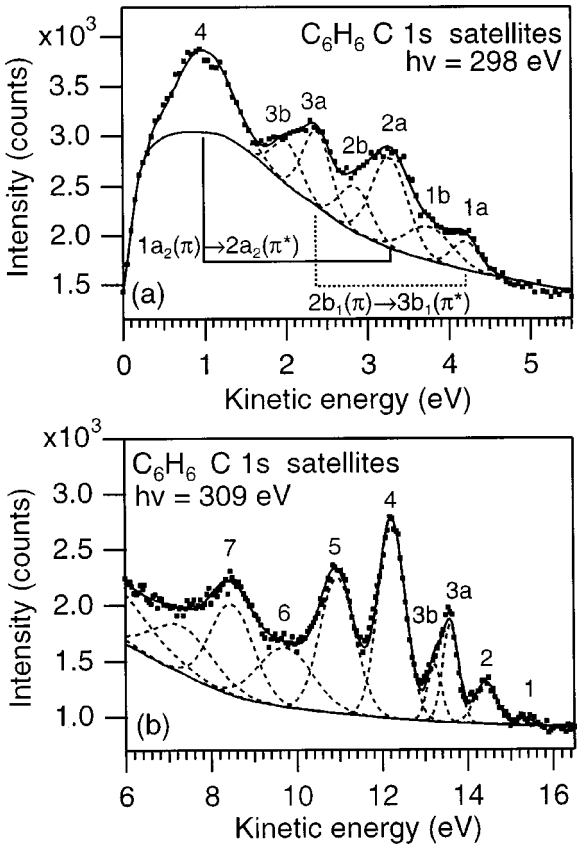

FIG. 9. The C 1*s* shake-up spectra of benzene taken at 298 eV (a) and 309 eV (b) photon energies. Total energy resolution was approximately 230 meV. The $2b_1(\pi)\rightarrow 3b_1(\pi^*)$ and $1a_2(\pi)\rightarrow 2a_2(\pi^*)$ exchange split transitions (Ref. 70) have been marked on (a).

IX. SHAKE-UP SATELLITES AND ANGULAR DISTRIBUTION

A number of theoretical and experimental[45,67–72] investigations of the C 1*s* shake-up satellites of benzene exist, although these concentrate mainly on the sudden limit energy region and are based on two photoelectron spectra recorded using Al Kα radiation.[45,69] The better resolved spectrum of Nordfors *et al.*[69] shows five satellite peaks with a binding energy approximately 5–11 eV relative to the main line. Theoretical calculations have allowed the first four satellite peaks to be assigned to $\pi-\pi^*$ excitations,[45,67,69,70] while the fifth was reassigned from a $\pi\rightarrow\pi^*$ (Refs. 45, 67, 69) to a $\sigma\rightarrow\sigma^*$ excitation (Ref. 70). Further weak satellite structures at higher binding energies overlap with a strong shake-off continuum and have not been described in the literature. Piancastelli *et al.*[3] investigated the photon energy-dependent behavior of the asymmetry parameter of the whole group of shake-up satellites.

Typical satellite spectra are displayed in Fig. 9. Figure 9(a) shows a spectrum 4 eV above the first satellite threshold and below the resonance ''b_1,'' while Fig. 9(b) shows a spectrum 15 eV above the first satellite threshold. The energies and satellite assignments along with previous results are summarized in Table II. Satellites 1*a* and 3*a* are of the correct energy to correspond to the respective triplet and singlet exchange split $2b_1(\pi)\rightarrow 3b_1(\pi^*)$ transitions and similarly satellites 2*a* and 4 correspond to the triplet (sat. 2*a*) and singlet (sat. 4) $1a_2(\pi)\rightarrow 2a_2(\pi^*)$ transitions.[50] The fact that 3*a* is assigned differently by Sjögren[67] is probably an expression of the general shortcoming of a single configuration description for the manifold of π-excited states, since in both Ref. 67 and Ref. 50 configuration interaction calculations using all single and double σ- and π-excitations have been performed. In most other respects the results are similar. In a more broad range theoretical study of the shake-up spectra of benzene and some benzene derivatives Yang and Ågren[72] reported assignments for the shake-up transitions which differ from the assignments included in Table II.

Figure 10 shows the photon energy dependent behavior of the satellites 1–5 and 7. A maximum near threshold is exhibited by the satellites 1–5 which correspond to $\pi\rightarrow\pi^*$ excitations, but not satellite by 7, which lends weight to the assignment of this satellite to a $\sigma\rightarrow\sigma^*$ transition.[70] This is contrary to the most recent calculations by Sjögren.[67] Similar behavior to that of satellites 1–5 (singlet and triplet $\pi\rightarrow\pi^*$ excitations) is exhibited by the S_0 (singlet $\pi\rightarrow\pi^*$) and S_1 (triplet $\pi\rightarrow\pi^*$) absolute satellite cross sections of the unsaturated molecules ethyne[19] and ethene.[12] In benzene the triplet $\pi\rightarrow\pi^*$ excitations, satellites 1 and 2, and one of the singlet $\pi\rightarrow\pi^*$ excitations, satellite 3, are enhanced near threshold and decrease strongly after a few eV indicating a conjugate contribution of their intensity. A conjugate shake-up transition consists of a dipole excitation of a core electron into an empty valence orbital and monopole ionization of valence electron. While conjugate processes play no role in the sudden limit, they can lead to a strong enhancement of certain satellites or to the appearance of additional satellite peaks near the ionization threshold. Although no evidence is seen for additional satellite peaks near threshold due to pure conjugate processes, the enhanced intensities of satellites 1, 2, and 3 indicate that conjugate contributions play an important role in the satellite structure of benzene.

The photon energy dependence of the benzene main line and satellite 4 asymmetry parameters β, along with the β parameter for the benzene C $1s^{-1}$ main line extracted from Piancastelli *et al.*[3] are shown in Fig. 11. For the error in the main line β we expect a fixed offset of less than ± 0.1 for imperfections in the symmetry of the apparatus, a multiplication of all values by a common factor between 0.96–1.04 resulting from the error in determination of the light polarization and a random contribution of 0.01 from statistics. The asymmetry parameter of the main line is relatively smooth in comparison to, for example, CO (Ref. 33) and N_2 (Ref. 31). However, this smooth behavior of the main line asymmetry parameter is also present in the most simple chain hydrocarbons C_2H_4,[12] C_2H_2,[19] and CH_4.[32]

The asymmetry parameters of the other satellites, including satellite 7 ($\sigma\rightarrow\sigma^*$), are similar to satellite 4 and hence are not shown.

In recent theoretical and experimental work an influence of nondipole terms in the photoionisation amplitudes well below 1 keV photon energy was suggested by Refs. 73–75, see also Ref. 76 for a review. These additional terms will have an influence on measurements conducted outside of the so-called dipole plane, i.e., the plane perpendicular to the

TABLE II. Binding energies of the benzene shake-up satellites. All satellite intensities are written as a percentage of the C 1*s* mainline.

	This work		Ref. 67			Refs. 45, 69, 70				
Satellite	Energy (eV)	Intensity (%) (323 eV)	Energy (eV) theory	Intensity (%) theory	Assignment state[spin]	Energy (eV) experiment[a]	Intensity (%) experiment	Energy (eV) theory[b]	Intensity (%) theory	Assignment
1*a*	3.9±0.1	0.16	4.07	⋯	1^T			4.14[c]	⋯	$^3[2b_1(\pi)\rightarrow 3b_1(\pi^*)]$
1*b*	4.2±0.1									
2*a*	4.8±0.1	0.83	4.40	⋯	2^T	4.8±0.1	0.3	4.66[c]	⋯	$^3[1a_2(\pi)\rightarrow 2a_2(\pi^*)]$
2*b*	5.2±0.1									
3*a*	5.8±0.1	2.21	5.36	4.8	2^s	5.8±0.1	2.8	5.54	4.6	$2b_1(\pi)\rightarrow 3b_1(\pi^*)$
3*b*	6.2±0.1									
4	7.15±0.05	5.52	6.47	8.9	3^s	7.0±<0.1	5.4	6.42	7.2	$1a_2(\pi)\rightarrow 2a_2(\pi^*)$
5	8.4±0.1	4.47	7.62	1.9	4^s	8.4±<0.1	4.0	9.45	4.6	$1b_1(\pi)\rightarrow 3b_1(\pi^*)$
6	9.8±0.2	2.01	9.89[d]	2.2	7^s					
7	10.9±0.1	3.42	10.89[d]	1.6	9^s	10.9±<0.1	2.9	12.46	0.7	$7b_2(\sigma)\rightarrow 8b_2(\sigma^*)$
8	12.0±0.5	1.43				13.4±0.3	⋯			
9	14.4±0.3	7.24				14.8±0.4	⋯			
10	16.7±0.3	3.13				16.6±0.3	⋯			
11						18.8±0.6	⋯			

[a]The experimental shake-up spectrum of Ref. 67 was measured with AlK_α *x*-ray radiation (1487 eV).
[b]The most advanced theoretical results of Lunell *et al.* (Ref. 70) are shown here, CISD calculations (configuration interaction between all singly and doubly excited $\sigma\rightarrow\sigma^*$ and $\pi\rightarrow\pi^*$ configurations).
[c]For the first two satellite peaks, values have not been given for the CISD calculation and we have taken the values from the CIS calculations (configuration interaction between all singly excited $\sigma\rightarrow\sigma^*$ and $\pi\rightarrow\pi^*$ configurations).
[d]Sjögren (Ref. 67) originally assigned satellite 7 to the calculated peak at 9.89 eV, however, this was based on the experimental results (Ref. 69) which failed to resolve satellite 6. Thus the calculated peak at 10.89 eV did not match with an experimental value.

light propagation vector. Since our analyzer accepts electrons scattered backward within a cone of 54.7° opening angle with respect to the light axis, these effects have to be considered. We will give a detailed treatment of the possible influence of these effects for our spectrometer in a forthcoming publication.[38] Here only the following result is of importance: Including the most important nondipole term, our measured angular distribution parameter, as depicted in Fig. 11, is denoted by β' and has to be written as $\beta' = (\beta - 2\gamma 3^{-3/2})$. Here β is the dipole angular distribution parameter and γ is defined as in Ref. 74. This will not influence the validity of the observations given in Fig. 11, but may of course alter their interpretation.

An assessment of the strength of multipole effects in this particular case for benzene can be made from the comparison of our measured angular distribution values with the results of Piancastelli *et al.*[3] (see Fig. 11). These were measured in a forward scattering geometry, where the influence of γ on the measured β' appears with a reversed sign. The deviations between the two curves are inside of the systematical errors quoted (±0.1 in the case of Ref. 3) for all but the lowest energies. For the first four data points of Piancastelli *et al.* the deviation is about 0.2. To explain this difference by quadrupole effects a γ of −0.26 is needed. This would lead to a 5% decrease in the cross section measured in Ref. 3, and the same increase in the cross section of this work, with respect to the true partial cross section (see Ref. 38 for details). These numbers are too small by far to explain the difference between the cross section curves of Ref. 3 and this work. Therefore, although this topic surely needs further investigation, at the moment we do not see evidence for strong multipole effects in this work.

X. CONCLUSION

We have investigated the C 1*s* photoabsorption and photoionization behavior of benzene. The vibrational fine structure on both inner-shell resonances and photoelectron lines is complicated by vibronic coupling between the different symmetry-adapted hole states. In the case of the photoionization spectrum, a definite interpretation of the vibrational structure cannot be given without theoretical guidance. From the geometry of the core-equivalent species, the excitation of at least the C–H stretching mode and one ring deformation mode is expected. A least-squares fit using two vibrational progressions, with the coupling strength for the C–H stretch given by the fully localized, building block model of Sæthre *et al.*[17] produced results compatible with the data. In contradiction to this model, however, introduction of a second vibrational mode has been vital in the ex-

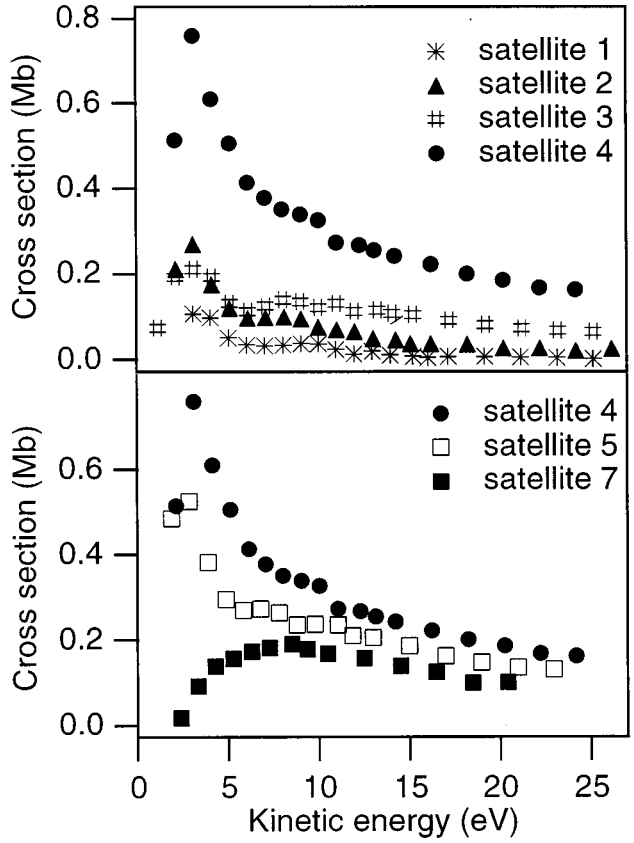

FIG. 10. The photon energy dependent behavior of the absolute cross section of benzene shake-up satellites 1–5 ($\pi \rightarrow \pi^*$ excitation) and 7 ($\sigma \rightarrow \sigma^*$).

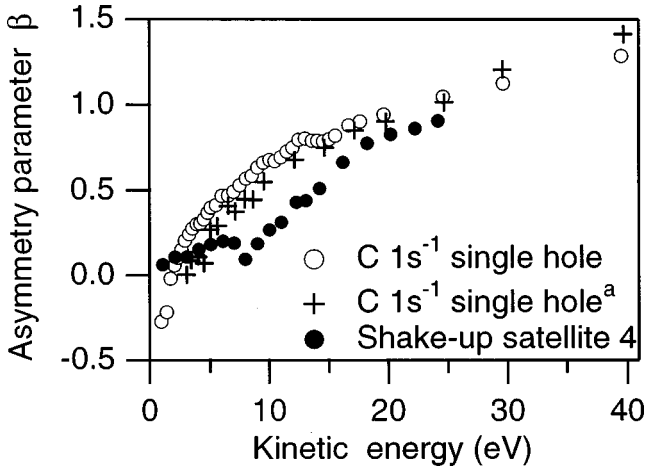

FIG. 11. The benzene main line (open dots) and satellite 4 (filled dots) asymmetry parameters extracted in a 54.7° backward scattering geometry. Results for the main line of Piancastelli *et al.* (Ref. 3) (forward scattering geometry) are included for comparison (crosses). All of the satellites have a very similar behavior to that of satellite 4 and hence are not shown.

planation of the spectrum. Whether this fact can be included in a localized model, or requires the use of a vibronic coupling theory, remains to be seen.

A break-down of the total photoabsorption cross section above the C 1*s* threshold into main line and satellite fractions of the cross section has revealed the major role of the satellites in producing the humps in the photoabsorption cross section usually assigned to the e_{2g} and a_{2g} shape resonances of benzene. Similar to the unsaturated hydrocarbon C_2H_2 we find that features in the photoabsorption cross section, undisputedly of σ-symmetry, turn out to be caused mainly by satellite excitations. Remnants of resonance effects in the main lines could still be found,[13,20] but on the whole these resonances are not single-particle phenomena. A connection between virtual molecular orbitals and the scattering picture, which is another way of rationalizing shape-resonances, has been made by Sheehy *et al.*, who showed the similarity of minimal basis set virtual orbitals to the continuum states of a square-well potential for simple molecules.[77] To stay in the scattering picture, our findings correspond to a large amplitude for inelastic scattering of emitted electrons on the surrounding atoms thereby giving rise to the excitation of satellite channels. This so-called direct knock-out effect has recently been worked out in some detail and underpinned with calculations for CO using a semiempirical optical potential.[78] The marked dip in the CO absorption cross section at 303 eV could thus be explained by the onset of satellite production. An alternative to this ansatz would be to extend the type of multichannel calculations that have recently been performed for valence ionization of ethyne to higher incident photon energies.[79] In a first multichannel scattering study of the C 1*s* ionization of ethyne published after the submission of the present work, this group[79] has shown a drastic decrease of the single channel shape resonance effect by taking satellite excitations into account.[80]

In a recent publication, single hole C 1*s* cross sections from multiple-scattering calculations have been given for condensed, oriented hydrocarbons.[59] Inelastic contributions have not been taken into account in this work. It is interesting to note that for ethyne, these data, if properly angle-averaged for an experiment on unoriented targets, are in perfect agreement with *the sum of the single hole and satellite contributions* to the total cross section, as derived from our work and Thomas *et al.*[7,20] Therefore, we suggest replacing the conclusion arrived at in Ref. 59, namely that satellite contributions do not play a role in C 1*s* photoemission from absorbed hydrocarbons, by a more plausible argument: Although the importance of satellite contributions in inner shell photoemission can undoubtedly be shown, certain aspects of this process are still amenable to a single particle description. It remains a subject of further theoretical and experimental studies to find out to what extent and why this simplified description can be recovered.

In an energy-dependent study of the benzene C 1*s* satellites we were able to show the importance of conjugate parts of the amplitude near threshold, a behavior which now appears to be quite common for hydrocarbons.[6,19,32]

ACKNOWLEDGMENTS

Discussions with H. Köppel are thankfully acknowledged. We are grateful for the financial support provided by the German Federal Ministry of Research and Technology (BMBF) and the Deutsche Forschungsgemeinschaft (DFG) for a postgraduate studentship (K. Maier). A.M.B. would like

to thank the Fonds der Chemischen Industrie for additional support. The National Synchrotron Light Source at Brookhaven National Laboratory is supported by the U.S. Department of Energy, Division of Material Sciences and Division of Chemical Sciences.

[1] B. Kempgens, H. M. Köppe, A. Kivimäki, M. Neeb, K. Maier, U. Hergenhahn, and A. M. Bradshaw, Surf. Sci. Lett. **425**, L376 (1999).
[2] E. E. Rennie, C. A. F. Johnson, J. E. Parker, D. M. P. Holland, D. A. Shaw, and M. A. Hayes, Chem. Phys. **229**, 107 (1998).
[3] M. N. Piancastelli, T. A. Ferrett, D. W. Lindle, L. J. Medhurst, P. A. Heimann, S. H. Liu, and D. A. Shirley, J. Chem. Phys. **90**, 3004 (1989).
[4] Y. Ma, F. Sette, G. Meigs, S. Modesti, and C. T. Chen, Phys. Rev. Lett. **63**, 2044 (1989).
[5] L. J. Medhurst, T. A. Ferrett, P. A. Heimann, D. W. Lindle, S. H. Liu, and D. A. Shirley, J. Chem. Phys. **89**, 6096 (1988).
[6] E. E. Rennie, H. M. Köppe, B. Kempgens, U. Hergenhahn, A. Kivimäki, K. Maier, M. Neeb, A. Rüdel, and A. M. Bradshaw, J. Phys. B **32**, 2691 (1999).
[7] B. Kempgens, H. M. Köppe, A. Kivimäki, M. Neeb, K. Maier, U. Hergenhahn, and A. M. Bradshaw, Phys. Rev. Lett. **79**, 35 (1997).
[8] S. J. Osborne, S. Sundin, A. Ausmees, S. Svensson, L. J. Sæthre, O. Svaeren, S. L. Sorensen, J. Végh, J. Karvonen, S. Aksela, and A. Kikas, J. Chem. Phys. **106**, 1661 (1997).
[9] T. D. Thomas, L. J. Sæthre, S. L. Sorensen, and S. Svensson, J. Chem. Phys. **109**, 1041 (1998).
[10] H. M. Köppe, A. L. D. Kilcoyne, J. Feldhaus, and A. M. Bradshaw, J. Chin. Chem. Soc. (Taipei) **42**, 255 (1995).
[11] M. Neeb, B. Kempgens, A. Kivimäki, H. M. Köppe, K. Maier, U. Hergenhahn, M. N. Piancastelli, A. Rüdel, and A. M. Bradshaw, J. Electron Spectrosc. Relat. Phenom. **88-91**, 19 (1998).
[12] B. Kempgens, A. Kivimäki, B. S. Itchkawitz, H. M. Köppe, M. Schmidbauer, M. Neeb, K. Maier, J. Feldhaus, and A. M. Bradshaw, J. Electron Spectrosc. Relat. Phenom. **93**, 39 (1998).
[13] S. L. Sorensen, M. Wiklund, S. Sundin, A. Ausmees, A. Kikas, and S. Svensson, Phys. Rev. A **58**, 1879 (1998).
[14] B. Kempgens, B. S. Itchkawitz, K. J. Randall, J. Feldhaus, A. M. Bradshaw, H. Köppel, F. X. Gadea, D. Nordfors, J. Schirmer, and L. S. Cederbaum, Chem. Phys. Lett. **246**, 347 (1995).
[15] D. M. P. Holland, D. A. Shaw, M. A. Hayes, L. G. Shpinkova, E. E. Rennie, L. Karlsson, P. Baltzer, and B. Wannberg, Chem. Phys. **219**, 91 (1997).
[16] J. Bozek, T. X. Carroll, J. Hahne, L. J. Sæthre, J. True, and T. D. Thomas, Phys. Rev. A **57**, 157 (1998).
[17] L. J. Sæthre, O. Sværen, S. Svensson, S. Osborne, T. D. Thomas, J. Jauhiainen, and S. Aksela, Phys. Rev. A **55**, 2748 (1997).
[18] B. Kempgens, B. S. Itchkawitz, J. Feldhaus, A. M. Bradshaw, H. Köppel, M. Döscher, F. X. Gadea, and L. S. Cederbaum, Chem. Phys. Lett. **277**, 436 (1997).
[19] B. Kempgens, A. Kivimäki, H. M. Köppe, M. Neeb, A. M. Bradshaw, and J. Feldhaus, J. Chem. Phys. **107**, 4219 (1997).
[20] T. D. Thomas, N. Berrah, J. Bozek, T. X. Carroll, J. Hahne, T. Karlsen, E. Kukk, and L. J. Sæthre, Phys. Rev. Lett. **82**, 1120 (1999).
[21] A. Kivimäki, B. Kempgens, K. Maier, H. M. Köppe, M. N. Piancastelli, M. Neeb, and A. M. Bradshaw, Phys. Rev. Lett. **79**, 998 (1997).
[22] N. V. Dobrodey, H. Köppel, and L. S. Cederbaum, Phys. Rev. A **60**, 1988 (1999), and references therein.
[23] H. D. Schulte and L. S. Cederbaum, J. Chem. Phys. **103**, 698 (1995).
[24] A. P. Hitchcock and C. E. Brion, J. Electron Spectrosc. Relat. Phenom. **10**, 317 (1977).
[25] A. P. Hitchcock, M. Pocock, C. E. Brion, M. S. Banna, D. C. Frost, C. A. McDowell, and B. Wallbank, J. Electron Spectrosc. Relat. Phenom. **13**, 345 (1978).
[26] D. Menzel, G. Rocker, H.-P. Steinrück, D. Coulman, P. A. Heimann, W. Huber, P. Zebisch, and D. R. Lloyd, J. Chem. Phys. **96**, 1724 (1992).
[27] J. A. Horsley, J. Stöhr, A. P. Hitchcock, D. C. Newbury, A. L. Johnson, and F. Sette, J. Chem. Phys. **83**, 6099 (1985).
[28] V. N. Akimov, A. S. Vinogradov, A. A. Pavlychev, and V. N. Sivkov, Opt. Spektrosk. **59**, 206 (1986) [Opt. Spectrosc.] **59**, 206 (1986).
[29] A. P. Hitchcock, P. Fischer, A. Gedanken, and M. B. Robin, J. Phys. Chem. **91**, 531 (1987).
[30] M. Schmidbauer, A. L. D. Kilcoyne, H. M. Köppe, J. Feldhaus, and A. M. Bradshaw, Phys. Rev. A **52**, 2095 (1995).
[31] B. Kempgens, A. Kivimäki, M. Neeb, H. M. Köppe, A. M. Bradshaw, and J. Feldhaus, J. Phys. B **29**, 5389 (1996).
[32] H. M. Köppe, B. S. Itchkawitz, A. L. D. Kilcoyne, J. Feldhaus, B. Kempgens, A. Kivimäki, M. Neeb, and A. M. Bradshaw, Phys. Rev. A **53**, 4120 (1996).
[33] H. M. Köppe, A. L. D. Kilcoyne, J. Feldhaus, and A. M. Bradshaw, J. Electron Spectrosc. Relat. Phenom. **75**, 97 (1995).
[34] E. Dietz, W. Braun, A. M. Bradshaw, and R. L. Johnson, Nucl. Instrum. Methods Phys. Res. A **239**, 359 (1985).
[35] K. J. Randall, J. Feldhaus, W. Erlebach, A. M. Bradshaw, W. Eberhardt, Z. Xu, Y. Ma, and P. D. Johnson, Rev. Sci. Instrum. **63**, 1367 (1992).
[36] B. S. Itchkawitz, B. Kempgens, H. M. Köppe, J. Feldhaus, A. M. Bradshaw, and W. B. Peatman, Rev. Sci. Instrum. **66**, 1531 (1995).
[37] J. Feldhaus, W. Erlebach, A. L. D. Kilcoyne, K. J. Randall, and M. Schmidbauer, Rev. Sci. Instrum. **63**, 1454 (1992).
[38] A. Kivimäki, U. Hergenhahn, B. Kempgens, R. Hentges, M. N. Piancastelli, K. Maier, A. Rüdel, J. J. Tulkki, and A. M. Bradshaw, Phys. Rev. B (submitted).
[39] M. Y. Kuchiev and S. A. Sheinerman, Sov. Phys. JETP **63**, 986 (1986).
[40] G. B. Armen, Phys. Rev. A **37**, 995 (1988).
[41] F. Wuilleumier, Adv. X-Ray Anal. **16**, 63 (1973).
[42] B. Kempgens, B. S. Itchkawitz, W. Erlebach, H. M. Köppe, J. Feldhaus, and A. M. Bradshaw (unpublished).
[43] B. L. Henke, P. Lee, T. J. Tanaka, R. L. Shimabukuro, and B. K. Fujikawa, At. Data Nucl. Data Tables **27**, 1 (1982).
[44] W. H. E. Schwarz, T. C. Chang, U. Seeger, and K. H. Hwang, Chem. Phys. **117**, 73 (1987).
[45] S. Lunell, S. Svensson, P. Å. Malmqvist, U. Gelius, E. Basilier, and K. Siegbahn, Chem. Phys. Lett. **54**, 420 (1978).
[46] O. Christiansen, J. F. Stanton, and J. Gauss., J. Chem. Phys. **108**, 3987 (1998).
[47] H. Köppel, F. X. Gadea, G. Klatt, J. Schirmer, and L. S. Cederbaum, J. Chem. Phys. **106**, 4415 (1997).
[48] M. W. Schmidt, K. K. Baldridge, J. A. Boatz, S. T. Elbert, M. S. Gordon, J. H. Jensen, S. Koseki, N. Matsunaga, K. A. Nguyen, S. Su, T. L. Windus, M. Dupuis, and A. J. Montgomery, Jr., J. Comput. Chem. **14**, 1347 (1993).
[49] A. Kivimäki, M. Neeb, B. Kempgens, H. M. Köppe, K. Maier, and A. M. Bradshaw, J. Phys. B **30**, 4279 (1997).
[50] M. Bader, J. Haase, K.-H. Frank, C. Ocal, and A. Puschmann, J. Phys. (Paris), Colloq. **8**, 491 (1986).
[51] H. M. Köppe, Ph.D. thesis, Technische Universität Berlin, 1995.
[52] J. Stöhr, in *X-ray Absorption: Principles, Applications, Techniques of EXAFS, SEXAFS, and XANES*, edited by R. Prins and D. Koningsberger (Wiley, New York, 1985).
[53] CRC Handbook of Chemistry and Physics, 76th ed. (CRC, Boca Raton, New York, London, Tokyo, 1995).
[54] B. P. Hollebone, A. T. Wen, T. Tyliszczak, and A. P. Hitchcock, J. Electron Spectrosc. Relat. Phenom. **51**, 661 (1990).
[55] J. Stöhr and K. R. Bauchspiess, Phys. Rev. Lett. **67**, 3376 (1991).
[56] F. Sette, J. Stöhr, and A. P. Hitchcock, J. Chem. Phys. **81**, 4906 (1984).
[57] M. N. Piancastelli, J. Electron Spectrosc. Relat. Phenom. **100**, 167 (1999).
[58] Y. F. Migal, J. Phys. B **27**, 1515 (1994); **32**, 4605 (1999), and references therein.
[59] N. Haack, G. Ceballos, H. Wende, K. Baberschke, D. Arvanitis, A. L. Ankudinov, and J. J. Rehr, Phys. Rev. Lett. **84**, 614 (2000).
[60] A. L. Ankudinov, B. Ravel, J. J. Rehr, and S. D. Conradson, Phys. Rev. B **58**, 7565 (1998).
[61] E. E. Rennie, U. Hergenhahn, H. M. Köppe, A. Kivimäki, M. Neeb, and A. M. Bradshaw (unpublished).
[62] K. Siegbahn, C. Nordling, G. Johansson, J. Hedman, P. F. Heden, K. Hamrin, U. Gelius, T. Bergmark, L. O. Werme, R. Manne, and Y. Baer, *Esca Applied to Free Molecules* (North Holland, Amsterdam, 1969).
[63] G. Bieri and L. Åsbrink, J. Electron Spectrosc. Relat. Phenom. **20**, 149 (1980).
[64] M. Schmidbauer, A. L. D. Kilcoyne, H. M. Köppe, J. Feldhaus, and A. M. Bradshaw, Chem. Phys. Lett. **199**, 119 (1992).
[65] P. Erman, A. Karawajczyk, U. Köble, E. Rachlew, K. Y. Franzén, and L. Veseth, Phys. Rev. Lett. **76**, 4136 (1996).
[66] R. R. Lucchese and F. A. Gianturco, Int. Rev. Phys. Chem. **15**, 429 (1996).
[67] B. Sjögren, J. Chem. Phys. **96**, 8338 (1992).
[68] T. Ohta, T. Fujikawa, and H. Kuroda, Chem. Phys. Lett. **32**, 369 (1975).

[69] D. Nordfors, A. Nilsson, N. Mårtensson, S. Svensson, U. Gelius, and S. Lunell, J. Chem. Phys. **88**, 2630 (1988).
[70] S. Lunell, M. P. Keane, and S. Svensson, J. Chem. Phys. **90**, 4341 (1989).
[71] R. W. Bigelow and H.-J. Freund, J. Chem. Phys. **77**, 5552 (1982).
[72] L. Yang and H. Ågren, Chem. Phys. **222**, 139 (1997).
[73] A. Bechler and R. H. Pratt, Phys. Rev. A **42**, 6400 (1990).
[74] J. W. Cooper, Phys. Rev. A **47**, 1841 (1993). Note that Eq. (23) of this work is not correct.
[75] O. Hemmers, G. Fisher, P. Glans, D. L. Hansen, H. Wang, S. B. Whitfield, R. Wehlitz, J. C. Levin, I. A. Sellin, R. C. C. Perera, E. W. B. Dias, H. S. Chakraborty, P. C. Deshmukh, S. T. Manson, and D. W. Lindle, J. Phys. B **30**, L727 (1997).
[76] D. W. Lindle and O. Hemmers, J. Electron Spectrosc. Relat. Phenom. **100**, 297 (1999).
[77] J. A. Sheehy, T. J. Gil, C. L. Winstead, R. E. Farren, and P. W. Langhoff, J. Chem. Phys. **91**, 1796 (1989).
[78] A. A. Pavlychev, J. Phys. B **32**, 2077 (1999).
[79] M. C. Wells and R. R. Lucchese, J. Chem. Phys. **110**, 9793 (1999); **111**, 6290 (1999).
[80] P. Lin and R. R. Lucchese, J. Chem. Phys. **113**, 1843 (2000).